Gait & Posture 125 (2026) 110070

Contents lists available at ScienceDirect

Gait & Posture

journal homepage: www.elsevier.com/locate/gaitpost

Medio-lateral forefoot segmentation for clinical gait analysis based on metatarsal subunit rigidity and angular motion

Amy B. Zavatsky [a,*], Po-Hsiang Chan [a], Julie Stebbins [b]

[a] Department of Engineering Science, University of Oxford, Oxford, UK
[b] Oxford Gait Laboratory, Nuffield Orthopaedic Centre, Oxford University Hospitals NHS Foundation Trust, Oxford, UK

ARTICLE INFO

Keywords:
Forefoot
Metatarsals
Multi-segment foot model
Rigidity
Gait analysis
Segmentation

ABSTRACT

Background: Although there is general agreement about the longitudinal division of the foot into segments for clinical gait analysis, there is limited evidence on which to base decisions about mediolateral segmentation, particularly in the metatarsal region.
Research question: We investigate how best to divide the metatarsals mediolaterally by considering both segment rigidity and angular motion.
Methods: Motion capture data were collected on 45 healthy adults during barefoot walking. The rigidities of ten subunits of adjacent metatarsals were quantified. Segment axes were defined for a selection of subunits and their three-dimensional angular motions calculated relative to an Oxford Foot Model (OFM) hindfoot segment.
Results: Subunits of metatarsals 2–3 and 3–4 were equally the most rigid, followed by subunit 2–3–4. Medial metatarsal groups were more rigid than lateral groups. Model A (metatarsal subunits 1–2–3 & 4–5), Model B (1–2 & 3–4–5), and Model C (1& 2–3–4 & 5) all had angular motion significantly different from the OFM forefoot for most of the gait cycle. There were significant differences between the motions of the medial and lateral subunits of Models A and B. The central subunit of Model C moved more like the medial subunits in dorsiflexion and more like the lateral subunits in adduction.
Significance: The forefoot models examined represent the minimum complexity required to capture metatarsal motion during walking. A mediolateral division of the forefoot at or adjacent to the third metatarsal is one option. The alternative is a three-segment model with a central subunit and separate first and fifth metatarsals.

1. Introduction

Multi-segment foot models (MFMs) [1] are used in gait analysis in conjunction with optical motion capture systems and lower-limb models to assess foot and ankle kinematics and kinetics. There is a wealth of evidence supporting the use of MFMs in clinical work for characterising gait disorders, planning treatment, and assessing outcomes [2–4].

The traditional, anatomical division of the foot in the longitudinal direction into tarsus, metatarsals, and phalanges is modified in most MFMs to be some combination of rearfoot (or hindfoot), midfoot, forefoot, and toe (or hallux) segments. This MFM partitioning is based not only on anatomy, but also on knowledge of foot kinematics and on grounds of practicality and repeatability in motion tracking. In the mediolateral direction, there is limited evidence on which to make decisions about segmentation, particularly in the metatarsal region. It is important to devise clinically relevant and viable ways to measure detailed metatarsal motion to aid in the treatment of pathologies that affect this region of the foot in particular, such as cerebral palsy [5], peripheral neuropathy [6], Charcot-Marie-Tooth disease [7], metatarsal stress fractures [8], and hallux valgus.

There are several possible ways to group the metatarsals into foot model segments. At one extreme, all five metatarsals can be gathered together as a single unit; at the other, each metatarsal can be modelled individually. Grouping metatarsals into subunits could be based on the relative motions of the tarsometatarsal joints, as is done in the separation of the foot into three 'columns': medial (medial cuneiform and first metatarsal), intermediate (middle and lateral cuneiforms and second and third metatarsals), and lateral (cuboid and fourth and fifth metatarsals) [9,10]. Some prefer to combine the medial and intermediate columns into a single functional unit [11], presumably based on the bony connections between the metatarsals and the hindfoot (the three medial metatarsals linking to the talus via the cuneiform-navicular

* Correspondence to: Botnar Institute for Musculoskeletal Sciences, Nuffield Orthopaedic Centre, Windmill Road, Oxford OX3 7LD, UK.
E-mail address: amy.zavatsky@eng.ox.ac.uk (A.B. Zavatsky).

https://doi.org/10.1016/j.gaitpost.2025.110070
Received 4 July 2025; Received in revised form 27 November 2025; Accepted 2 December 2025
Available online 4 December 2025

complex and the two lateral metatarsals connecting to the calcaneus via their articulations with the cuboid). Alternatively, a division could be related to the measured motions of individual metatarsals and neighbouring bones [12,13].

All MFMs include a forefoot, but the underlying bones which it represents vary from model to model [1]. Some MFMs combine a selection of midfoot bones with the metatarsals into a single forefoot segment (Milwaukee [14], Bruening [15]), while others include only the metatarsals (Oxford [16], Rizzoli [17]). Splitting the metatarsals into medial and lateral subunits is done as standard in some models (MacWilliams [18]) and as an option in others (Amsterdam [19]). There is no consensus as to where the dividing line should be or whether the first metatarsal should be separate. This is understandable, given the different applications of the models (targeted research, clinical work in general, or assessment of specific populations) and the challenge of repeatably placing and accurately tracking markers in close proximity on the foot.

In this study, we take a combined approach to forefoot segmentation and investigate how to divide the metatarsals mediolaterally based on metatarsal subunit rigidity and angular motion. Our aim is to devise a model with the minimum complexity necessary to capture metatarsal motion for clinical gait analysis. Our criteria for segmentation are based, firstly, on grouping together the metatarsals that are most rigidly associated with each other, and, secondly, on ensuring that there is distinct and clinically meaningful motion between the different parts of the forefoot.

2. Methods

Motion data were collected from 45 healthy adult volunteers (age 28.2 ± 6.8 years; 25 males, 20 females) with no known foot injuries or deformities using a motion capture system (16 Vicon T40 camera, Vicon Motion Systems Ltd., Oxford, UK) operating at 100 Hz. The study was approved by the University of Oxford Interdivisional Research Ethics Committee (R57227/RE001), and all participants gave informed consent to participate. Subjects posed in a static standing position and then walked barefoot in a straight line at self-selected speed. Motion tracking using markers for the Oxford Foot Model (OFM) [16,20] showed that foot kinematics were similar to those in the reference adult database of our clinical gait laboratory. As in Chan et al. [21], one representative trial of the six collected was selected for analysis (right leg only) using a root mean square error criterion.

To track the detailed movement of the forefoot bones, ten retroreflective passive markers (10 mm diameter) were attached to the skin at the proximal and distal ends of all five metatarsals (Fig. 1). Ten subunits of the forefoot were defined: four representing two adjacent metatarsals, three representing three adjacent metatarsals, two representing four adjacent metatarsals, and one representing all five metatarsals. Each subunit was tracked using a cluster of four markers, chosen to be those at the medial and lateral extremes of the subunit. For example, forefoot subunit 1–2 had tracking markers on metatarsals 1 and 2, and forefoot subunit 1–2–3 had tracking markers on metatarsals 1 and 3. Marker gap filling and trajectory filtering were done using Vicon Nexus (v2.3). Any trials with gaps larger than 15 frames (0.15 s) were discarded. Marker trajectories were exported to Matlab (R2017a & vR2023a, MathWorks, Inc., Natick, MA, USA) for all subsequent calculations.

The rigidity of each forefoot subunit was quantified using the rigid body error (σ_{RBE}) [21-24] calculated at each time frame of one representative gait cycle per participant. σ_{RBE} measures how well the tracking marker configuration at each time point compares to a specific pose (taken here to be 50 % stance [21]). The average σ_{RBE} quantifies the overall relative rigidity of a segment over one full gait cycle. If $\sigma_{RBE} = 0$, then the markers have not moved relative to each other at all during motion. Any increase in σ_{RBE} from zero indicates that the cluster of tracking markers has changed shape from its reference configuration,

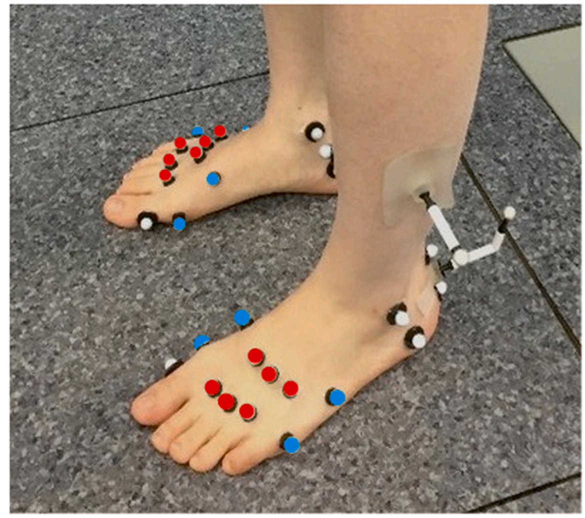

Fig. 1. Motion capture markers used in the study. Markers (indicated as blue circles) were placed on the medial and lateral aspects, respectively, of the bases and heads of the first and fifth metatarsals. For the other three metatarsals, markers (identified by red circles) were placed on the dorsal aspect of the foot, with distal markers located on the heads of the bones and proximal markers sited just distal to the bases of the bones. This was done to ensure that metatarsal motion, rather than a combination of metatarsal and mid-foot motion, was tracked. The white and blue markers on the feet are part of the standard OFM marker set; the OFM marker mid-way between the 2nd and 3rd metatarsal heads is not included here. A tibial 'wand' marker on the left leg is also visible.

and therefore more deformable marker clusters have higher values of σ_{RBE}. Equations for the calculation of σ_{RBE} are reproduced in Appendix A.

Potential forefoot models with mediolateral subdivisions were identified based on the σ_{RBE} results. Orthogonal segment axes were defined from the positions of the tracking markers on the metatarsal subunits (Fig. 2) and used to calculate their three-dimensional angular motions relative to an OFM hindfoot segment. For each forefoot segment, the *z*-axis was directed along a vector from the mid-point of the line segment connecting the two proximal markers to the mid-point of the line segment connecting the two distal markers. The *x*-axis was perpendicular to the plane defined by a vector connecting the two distal markers and a vector along the *z*-axis. The direction of the *y*-axis was mutually perpendicular to the other two axes. Joint angles were calculated according to a *YXZ* Euler sequence: dorsiflexion-plantarflexion about the mediolateral *y*-axis of the OFM hindfoot segment, abduction-adduction about a floating *x*-axis, and supination-pronation about the *z*-axis of the metatarsal segment.

Average σ_{RBE}s were tested for normality (Kolmogorov-Smirnov and Shapiro-Wilk tests), and all were found to be significantly different from a normal distribution. The averages were therefore compared across metatarsal subunits using the non-parametric Kruskal-Wallis and Mann-Whitney U tests. Segment angles over the gait cycle with average offsets removed were assessed using statistical parametric mapping (one-way repeated-measures ANOVA, followed by post-hoc two-tailed paired *t*-tests, alpha = 0.05) [25,26]. Since the results using parametric and non-parametric tests were found to be qualitatively the same, comparable to the biomechanical trajectory data analysed in [27, Fig. 7], for brevity, only the results from the parametric tests are reported here.

3. Results

The average σ_{RBE} (Fig. 3) was significantly different between forefoot subunits ($p < 0.01$). The five-metatarsal unit was the least rigid (most flexible) overall; subunits 2–3 and 3–4 were the most rigid, followed by subunit 2–3–4. The medial metatarsal groups were more rigid than the lateral groups. The changes in σ_{RBE} over the gait cycle for all subunits

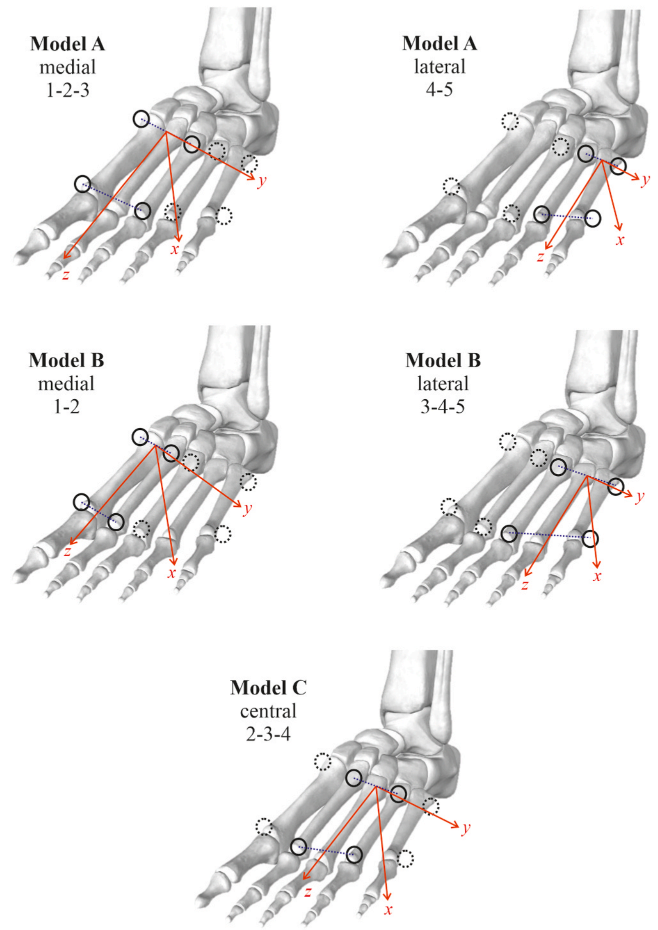

Fig. 2. Potential forefoot models. (Top row) Model A, with medial (1−2−3) and lateral (4−5) metatarsal subunits. (Middle row) Model B, with medial (1−2) and lateral (3−4−5) metatarsal subunits. (Bottom row) Model C, with central (2−3−4) metatarsal subunit.

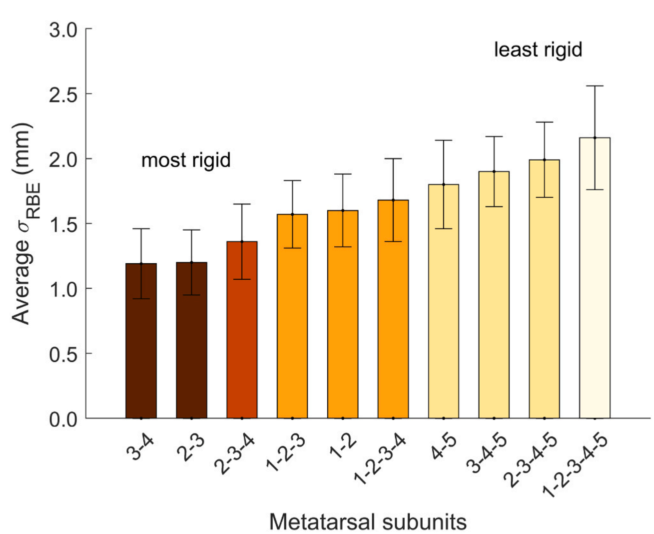

Fig. 3. Average σ_{RBE} for each metatarsal subunit ($n = 45$ feet) with ±1 standard deviation (mm) indicated. The lower the σ_{RBE}, the more rigid the subunit. Bars of the same colour indicate subunits with average σ_{RBE} values that are not significantly different ($p > 0.01$).

followed patterns similar to that for the OFM forefoot in Chan et al. [21, Fig. 3].

Since metatarsals 2 and 4 were more rigidly linked to metatarsal 3 than to metatarsals 1 and 5, the three-segment metatarsal subdivision 1 & 2–3–4 & 5 (Model C) is the best option based solely on the rigidity criterion. The two-segment mediolateral subdivisions 1–2–3 & 4–5 (Model A) and 1–2 & 3–4–5 (Model B) were also deemed to be worthy of investigation as they also represent metatarsal groups with low σ_{RBE} but require fewer motion-tracking markers than the three-segment model. Models A and B are essentially equivalent on the grounds of rigidity since it is not possible to say whether metatarsal 3 is more rigidly linked to the medial or the lateral metatarsals.

All segments of Models A, B, and C with two or more metatarsals had patterns of angular motion relative to the OFM hindfoot that were significantly different from the OFM forefoot segment for nearly all of the gait cycle (Supplementary material). The medial segments of Models A and B behaved similarly to each other in dorsiflexion-plantarflexion, supination-pronation, and abduction-adduction (Fig. 4, left), as did their lateral segments (Fig. 4, right). Much more noticeable and significant were the differences in angular motion found between the medial and lateral segments of both Model A and Model B (Fig. 5). Their motion patterns were similar in dorsiflexion-plantarflexion and supination-pronation, with the medial segment having a larger range of motion in the former and a smaller range of motion in the latter (Fig. 5, rows 1–2). The medial segment adducted more than the lateral segment in early stance (Fig. 5, row 3). After returning to a similar orientation in mid-stance, their paths diverged from approximately 45–75 % of the gait cycle (late stance through early swing), with the medial segment abducting and then adducting and the lateral segment doing the opposite. The central segment of Model C moved more like the medial segments of Models A and B in dorsiflexion-plantarflexion and more like their lateral segments in abduction-adduction (comparison with Model A only in Fig. 6 since Models A and B behaved similarly). Significant differences were identified in all angular rotations.

4. Discussion

This study took a combined approach to forefoot segmentation for MFMs by investigating how to divide the metatarsals mediolaterally based on metatarsal subunit rigidity and angular motion. The rigidity of ten combinations of adjacent metatarsals was quantified and the results used to identify three forefoot models for further examination. Their angular motions relative to a hindfoot segment were compared. Although some differences between the rigidity and motion of the subunits of the two-segment models (Models A and B) were evident, for practical purposes, the models might be considered to be indistinguishable. Therefore, a mediolateral division of the forefoot at the third metatarsal or on either side of it seems reasonable. The central metatarsal subunit of the three-segment model (Model C) was significantly more rigid than the subunits comprising the two-segment models. Its angular motion showed characteristics of both the medial and lateral segments of those models. Model C also allows for separate tracking of the first and fifth metatarsals, if needed.

It is important to acknowledge that the rigidity measure applied in this study (σ_{RBE}) captures both the soft-tissue movement and the flexibility of the segment due to bone movement. Furthermore, a marker cluster could remain rigid ($\sigma_{RBE} = 0$) yet still move independently from the underlying bone. Nonetheless, all average σ_{RBE} values in Fig. 2 were larger than previously reported inter-trial, inter-rater, and intra-rater repeatability errors of σ_{RBE} in the forefoot region [21, Appendix A], which lends credence to their use for comparing metatarsal subunits. It is recognized, however, that the earlier study [21] included only the standard OFM marker set and that training is likely needed for markers to be placed accurately and consistently on the central metatarsals, particularly at the proximal ends (P.-H. Chan, Motion Tracking and Modelling of the Forefoot for Clinical Gait Analysis, D.Phil. thesis,

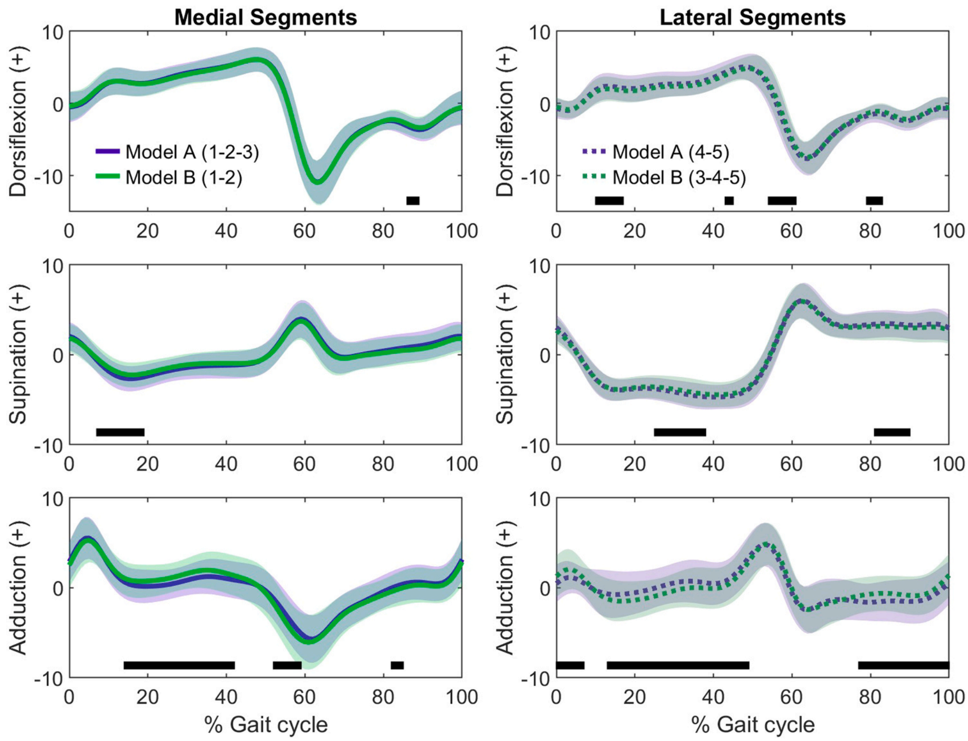

Fig. 4. Comparison of medial segment (left) and lateral segment (right) motions of Model A (purple) and Model B (green) over the gait cycle. Angular offsets removed; angles in degrees. (Top row) Dorsiflexion-plantarflexion. (Middle row) Supination-pronation. (Bottom row) Adduction-abduction. Black horizontal bars indicate periods in the gait cycle where significant differences between the curves were found.

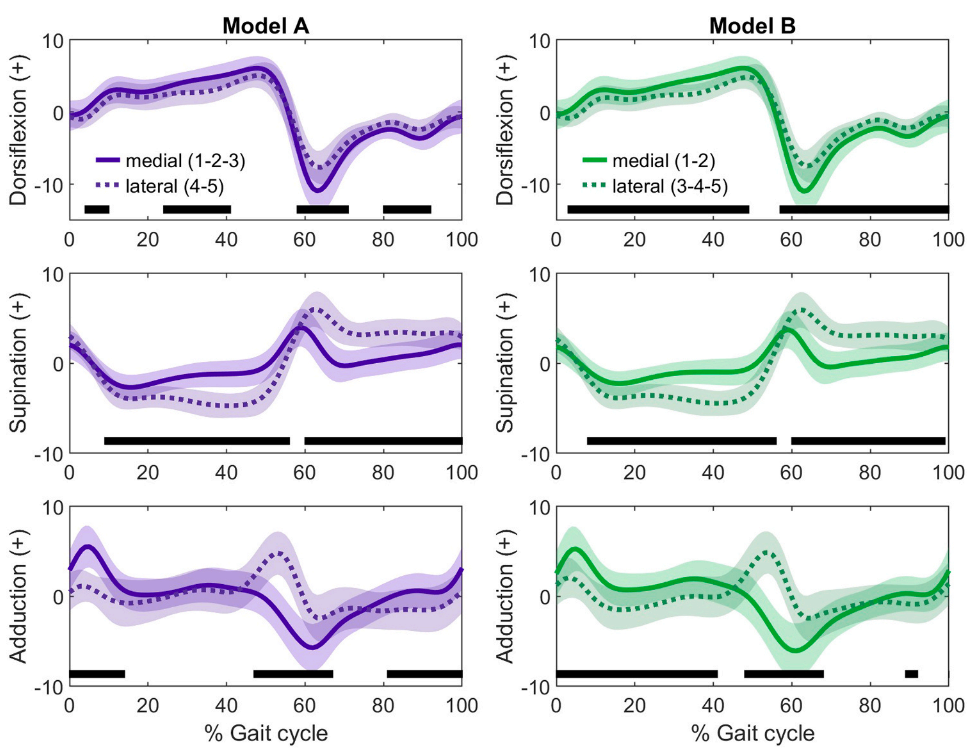

Fig. 5. Comparison of the angular motions of the medial segments (solid lines) and lateral segments (dotted lines) of Model A (left) and Model B (right) over the gait cycle. Angular offsets removed; angles in degrees. (Top row) Dorsiflexion-plantarflexion. (Middle row) Supination-pronation. (Bottom row) Adduction-abduction. Black horizontal bars indicate periods in the gait cycle where significant differences between the curves were found.

University of Oxford, 2019). It is also worth noting that the results presented here are based on healthy adults only and that further investigation may be required to apply the results with confidence to children, older adults, and patients with foot pathology. Body mass index and, to a lesser extent, gender are known to influence dynamic foot morphology [28], although there is no consensus in the literature on

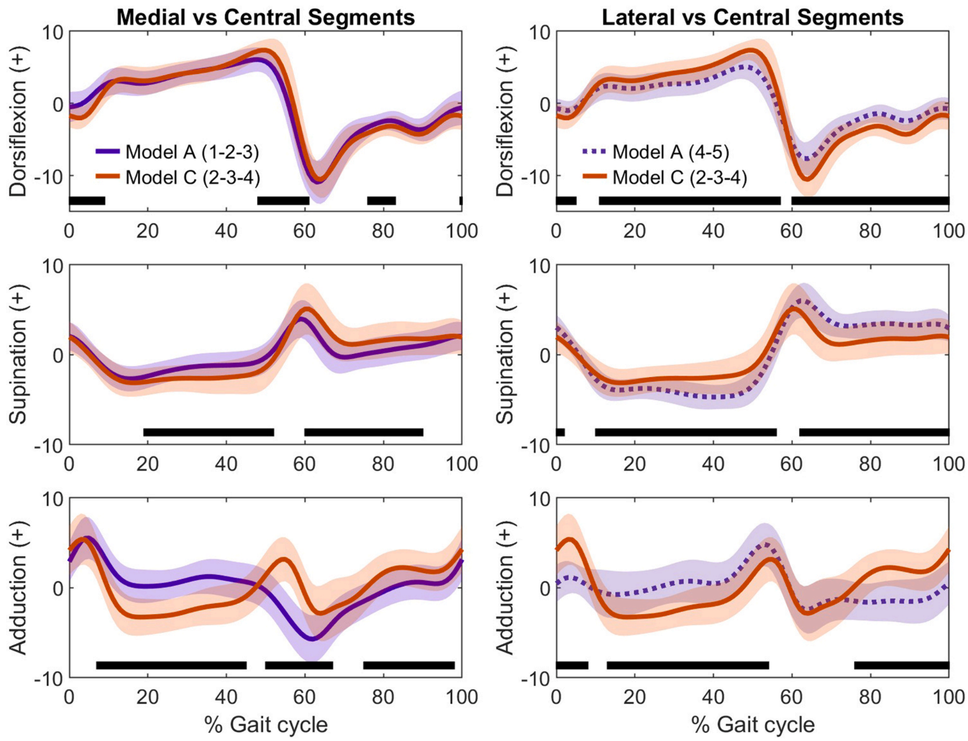

Fig. 6. Comparison of the angular motions of the medial (left) and lateral (right) segments of Model A (purple) and the central segment of Model C (orange) over the gait cycle. Angular offsets removed; angles in degrees. (Top row) Dorsiflexion-plantarflexion. (Middle row) Supination-pronation. (Bottom row) Adduction-abduction. Black horizontal bars indicate periods in the gait cycle where significant differences between the curves were found.

the precise links with foot kinematics. It should be noted, however, that no statistically significant effects of gender on average rigid-body error were found in our previous study [21]. In addition, the results here apply only to barefoot walking in a straight line at a self-selected speed on level ground.

It is difficult to compare our results directly to previous work, given the differences in experimental methodologies and study participants. Nonetheless, the results presented here are broadly consistent with the conclusions of others. Nester [29] reviewed dynamic cadaver and invasive in-vivo bone pin studies of foot motion, which suggest that the first, second, and third metatarsals are functionally distinct from the fourth and fifth metatarsals, with the latter moving consistently more during stance. Medial metatarsal motion was measured relative to the medial, central, and lateral cuneiforms, while lateral metatarsal motion was tracked relative to the cuboid. Additional motion between the cuboid and calcaneus served to increase the apparent mobility of the lateral side of the foot. In the present work, metatarsal motion is reported relative to the OFM hindfoot, not to the neighbouring midfoot bones, but our results still show differences in the ranges and patterns of motion between the two sides of the foot, with a larger range of supination for the lateral metatarsal groups (Fig. 5).

DiLiberto et al. [13] used skin-mounted electromagnetic trackers to measure the motion of the first, third, and fifth metatarsals relative to the calcaneus. They found the motion of the third metatarsal in the frontal and transverse planes to be more closely correlated to the motion of the fifth metatarsal than to the first. In the sagittal plane, strong couplings existed both between the third and first metatarsal and the third and fifth metatarsal. Also identified were differences in terminal stance phase angular excursions between the individual metatarsals and a unified forefoot, along with variations in motion coupling over the gait cycle. The authors suggested that a single forefoot segment might be adequate if only sagittal plane motion is of interest. If not, they recommended modelling the medial and lateral sides of the foot separately. Our results are also not conclusive as to whether the third metatarsal is more closely linked to the two medial or two lateral metatarsals (Fig. 3). Furthermore, we agree that a single forefoot segment should be adequate for applications requiring only plantar-dorsiflexion, but that a two-segment forefoot would be a valuable MFM option if three-dimensional forefoot motion is required (Fig. 5 and Supplementary material).

For the purposes of the present study, we removed static offsets from the data to enable easy comparisons of motion patterns between different representations of the forefoot. It is often important, however, to know the true relative positions of the foot segments, for example, the plantar-dorsiflexion of the medial metatarsals in comparison to the lateral ones. Therefore, reporting the angular motion results without removing offsets should be an option.

Although assessment of rigidity and distinct angular motion suggests the minimum complexity required to capture anatomically relevant motion of the forefoot, deciding on the most appropriate MFM for clinical gait analysis involves multiple, potentially conflicting, factors to be considered, including the reason for the assessment, the type of pathology being investigated (Charcot-Marie-Tooth Disease, for example, in which the distinct function of the 1st metatarsal may be of clinical interest), the technical capabilities of the motion tracking system, the practicality and repeatability of marker placement, and any relevant standards or recommendations from professional bodies [30]. In addition, backwards compatibility with historical data may be desirable, or even essential, for continuity of clinical work. Future work could also include investigation of other modelling approaches that do not require the assumption of rigid segments, to better describe the natural behaviour of the foot.

The review by Nester et al. [29] concluded that the high heterogeneity in foot structure and function should be seen as ‘an opportunity to develop patient-specific clinical models of foot function’. The findings of our study provide possible modelling options for the forefoot if marker placements and angle conventions similar to ours can be used. It would be reasonable to track the forefoot as one (central) segment for sagittal plane and frontal plane motion (plantar-dorsiflexion and pronation-supination) and potentially also useful to calculate the offset between medial and lateral segments in the sagittal plane. For studying pathologies involving individual metatarsals, the directions of the first and fifth metatarsals could be calculated, although a decision would have to be made as to the most clinically meaningful ways to report these. If full three-dimensional motion or transverse plane motion (abduction-adduction) is of interest, the forefoot could be split into medial and lateral segments at or adjacent to the third metatarsal. Further studies of feet with pathologies routinely seen in clinical gait laboratories are needed to decide which forefoot modelling options are best for a particular patient group.

CRediT authorship contribution statement

Po-Hsiang Chan: Writing – review & editing, Writing – original draft, Validation, Software, Methodology, Investigation, Formal analysis, Data curation. **Amy B. Zavatsky:** Writing – review & editing, Writing – original draft, Visualization, Supervision, Methodology, Formal analysis, Conceptualization. **Julie Stebbins:** Writing – review & editing, Writing – original draft, Visualization, Validation, Supervision, Resources, Methodology, Investigation, Formal analysis, Data curation, Conceptualization.

Funding sources

This research was not funded by any specific grant from funding agencies in the public, commercial, or not-for-profit sectors.

Declaration of Competing Interest

The authors declare that there are no conflicts of interest in the present study.

Acknowledgements

The authors would like to thank the team at the Oxford Gait Laboratory for their assistance with this study.

Appendix A. Supporting information

Supplementary data associated with this article can be found in the online version at doi:10.1016/j.gaitpost.2025.110070.

References

[1] A. Stone, Multisegment foot models, in: W.R. Ledoux, S. Telfer (Eds.), Foot and Ankle Biomechanics, Academic Press, Cambridge, Massachusetts, USA, 2023, pp. 151–165, https://doi.org/10.1016/C2017-0-03286-X.

[2] A. Leardini, P. Caravaggi, T. Theologis, J. Stebbins, Multi-segment foot models and their use in clinical populations, Gait Posture 69 (2019) 50–59, https://doi.org/10.1016/j.gaitpost.2019.01.022.

[3] K. Deschamps, F. Staes, P. Roosen, F. Nobels, K. Desloovere, H. Bruyninckx, et al., Body of evidence supporting the clinical use of 3D multisegment foot models: a systematic review, Gait Posture 33 (2011) 338–349, https://doi.org/10.1016/j.gaitpost.2010.12.018.

[4] L. Rankine, J. Long, K. Canseco, G. Harris, Multisegmental foot modeling: a review, Crit. Rev. Biomed. Eng. 36 (2008) 127–181, https://doi.org/10.1615/CritRevBiomedEng.v36.i2-3.30.

[5] P. Kedem P, D.M. Scher, Foot deformities in children with cerebral palsy, Curr. Opin. Pediatr. 27 (2015) 67–74, https://doi.org/10.1097/MOP.0000000000000180.

[6] J.S. Wrobel, B. Najafi, Diabetic foot biomechanics and gait dysfunction, J. Diabetes Sci. Technol. 4 (2010) 833–845, https://doi.org/10.1177/193229681000400411.

[7] J.R. Holmes, S.T. Hansen, Foot and ankle manifestations of charcot-marie-tooth disease, Foot Ankle 14 (1993) 476–486, https://doi.org/10.1177/107110079301400809.

[8] J.C. Mandell, B. Khurana, S.E. Smith, Stress fractures of the foot and ankle, part 1: biomechanics of bone and principles of imaging and treatment, Skelet. Radiol. 46 (2017) 1021–1029, https://doi.org/10.1007/s00256-017-2640-7.

[9] M.N. Mojica, J.S. Early, Foot Biomechanics, in: J.B. Webster, D.P. Murphy (Eds.), Atlas of Orthoses and Assistive Devices, (Fifth Edition), Elsevier, 2019, pp. 216–228.e1, https://doi.org/10.1016/B978-0-323-48323-0.00019-6.

[10] A.S. Kelikian, S.K. Sarrafian, Sarrafin's Anatomy of the Foot and Ankle: Descriptive. Topographic, Functional, Lippincott Williams & Wilkins, 2011.

[11] J.R. Davids, J. Shilt, R. Kay, T. Dreher, B.J. Shore, J. McCarthy, W. Shrader, K. Graham, M. Veerkamp, U. Narayanan, H. Chambers, T. Novacheck, J. Rhodes, A. Van Campenhout, K. Pierz, T. Theologis, E. Rutz, Assessment of foot alignment and function for ambulatory children with cerebral palsy: results of a modified Delphi technique consensus study, J. Child. 's. Orthop. 16 (2022) 111–120, https://doi.org/10.1177/18632521221084183.

[12] P. Wolf, A. Stacoff, A. Liu, C. Nester, A. Arndt, A. Lundberg, et al., Functional units of the human foot, Gait Posture 28 (2008) 434–441, https://doi.org/10.1016/j.gaitpost.2008.02.004.

[13] F.E. DiLiberto, J. Tome, J.F. Baumhauer, J. Houck, D.A. Nawoczenski, Individual metatarsal and forefoot kinematics during walking in people with diabetes mellitus and peripheral neuropathy, Gait Posture 42 (2015) 435–441, https://doi.org/10.1016/j.gaitpost.2015.07.012.

[14] S.M. Kidder, F.S. Abuzzahab, G.F. Harris, J.E. Johnson, J.E, A system for the analysis of foot and ankle kinematics during gait, IEEE Trans. Rehabil. Eng. 4 (1996) 25–32, https://doi.org/10.1109/86.486054.

[15] D.A. Bruening, K.M. Cooney, F.L. Buczek, Analysis of a kinetic multi-segment foot model. Part I: model repeatability and kinematic validity, Gait Posture 35 (2012) 529–534, https://doi.org/10.1016/j.gaitpost.2011.11.012.

[16] J. Stebbins, M. Harrington, N. Thompson, A. Zavatsky, T. Theologis, Repeatability of a model for measuring multi-segment foot kinematics in children, Gait Posture 23 (2006) 401–410, https://doi.org/10.1016/j.gaitpost.2005.03.002.

[17] A. Leardini, M.G. Benedetti, L. Berti, D. Bettinelli, R. Nativo, S. Giannini, S, Rear-foot, mid-foot and fore-foot motion during the stance phase of gait, Gait Posture 25 (2007) 453–462, https://doi.org/10.1016/j.gaitpost.2006.05.017.

[18] B.A. MacWilliams, M. Cowley, D.E. Nicholson, Foot kinematics and kinetics during adolescent gait, Gait Posture 17 (2003) 214–224, https://doi.org/10.1016/S0966-6362(02)00103-0.

[19] W. Schallig, J.C. van den Noort, M. Piening, G.J. Streekstra, M. Maas, M.M. van der Krogt, J. Harlaar, The Amsterdam foot model: a clinically informed multi-segment foot model developed to minimize measurement errors in foot kinematics, J. Foot Ankle Res. 15 (2022) 46, https://doi.org/10.1186/s13047-022-00543-6.

[20] P.C. Dixon, E.E. Drew, S.P. McBride, M. Harrington, J. Stebbins, A.B. Zavatsky, openOFM: an open-source implementation of the multi-segment Oxford Foot Model, Comput. Methods Biomech. Biomed. Eng. (2024), https://doi.org/10.1080/10255842.2024.2448558. 〈〉.

[21] P.-H. Chan, J. Stebbins, A.B. Zavatsky, Marker cluster rigidity in a multi-segment foot model, J. Biomech. 84 (2019) 284–289, https://doi.org/10.1016/j.jbiomech.2018.12.045.

[22] I. Söderkvist, P.Å. Wedin, Determining the movements of the skeleton using well-configured markers, J. Biomech. 26 (1993) 1473–1477, https://doi.org/10.1016/0021-9290(93)90098-Y.

[23] A.J. van den Bogert, G.D. Smith, B.M. Nigg, In vivo determination of the anatomical axes of the ankle joint complex: an optimization approach, J. Biomech. 27 (1994) 1477–1488, https://doi.org/10.1016/0021-9290(94)90197-X.

[24] P.-H. Chan, J. Stebbins, A.B. Zavatsky, Efficacy of quantifying marker-cluster rigidity in a multi-segment foot model: a Monte-Carlo based global sensitivity analysis and regression model, Comput. Methods Biomech. Biomed. Eng. 25 (2021) 308–319, https://doi.org/10.1080/10255842.2021.1954170.

[25] T.C. Pataky, Generalized *n*-dimensional biomechanical field analysis using statistical parametric mapping, J. Biomech. 43 (2010) 1976–1982, https://doi.org/10.1016/j.jbiomech.2010.03.008. 〈〉.

[26] T.C. Pataky, One-dimensional statistical parametric mapping in Python, Comp. Meth. Biomech. Biomed. Eng. 15 (2012) 295–301, https://doi.org/10.1080/10255842.2010.527837.

[27] T.C. Pataky, J. Vanrenterghem, M.A. Robinson, Zero- vs. one-dimensional, parametric vs. non-parametric, and confidence interval vs. hypothesis testing procedures in one-dimensional biomechanical trajectory analysis, J. Biomech. 48 (2015) 1277–1285, https://doi.org/10.1016/j.jbiomech.2015.02.051.

[28] B. Fritz, T. Schmeltzpfenning, C. Plank, T. Hein, S. Grau, Anthropometric influences on dynamic foot shape: measurements of plantar three-dimensional foot deformation, Footwear Sci. 5 (2013) 121–129, https://doi.org/10.1080/19424280.2013.789559.

[29] C.J. Nester, Lessons from dynamic cadaver and invasive bone pin studies: do we know how the foot really moves? J. Foot Ankle Res. 9 (2009) 18, https://doi.org/10.1186/1757-1146-2-18.

[30] A. Leardini, J. Stebbins, H. Hillstrom, P. Caravaggi, K. Deschamps, A. Arndt, ISB recommendations for skin-marker-based multi-segment foot kinematics, J. Biomech. 125 (2021) 110581, https://doi.org/10.1016/j.jbiomech.2021.110581.